ELECTRONIC SUPPORTING INFORMATION

Uncharted Waters – Determining the influence of polar solutes on lanthanide solvent extraction by hydrophobic eutectic solvents

Rodrigo Colhe[a], Amélie Tropres[b], Maísa Saldanha Pinheiro[a], Thaís S. Soares,[c] Takafumi Hanada[d], Duarte Ananias[a], Felipe Olea[a], Inês Vaz [a], João A.P. Coutinho[a], Nicolas Schaeffer[a*]

[a]CICECO - Aveiro Institute of Materials, Department of Chemistry, University of Aveiro, 3810-193 Aveiro, Portugal

[b] Université Claude Bernard, 69622 Villeurbanne, Lyon, France

[c] Group of Analysis and Education for Sustainability (GAES), Chemistry Department, Federal University of Viçosa (UFV), Viçosa, MG 36570–900, Brazil

[d] Department of Applied Chemistry, Graduate School of Technology, Industrial and Social Sciences, Tokushima University, 2-1 Minamijosanjima, Tokushima 770-8506, Japan

* Corresponding email: nicolas.schaeffer@ua.pt

PHASE DIAGRAM

Table S1. Experimental (x_{TOPO}, T) and calculated (γ_i) data of the SLE of systems involving trioctylphosphine oxide (TOPO) with acetic acid (AceA) or hexanoic acid (HexA).

HBD	**AceA**			**HexA**		
x_{TOPO}	T (K)	$\gamma_{e,TOPO}$	$\gamma_{e,HBD}$	T (K)	$\gamma_{e,TOPO}$	$\gamma_{e,HBD}$
0.0	289.8	1.00	-	269.20	1.00	-
0.1	277.28	0.89	-	263.68	0.95	-
0.2	264.46	0.78	-	254.11	0.81	-
0.3	249.65	0.65	0.02	244.78	0.69	0.01
0.4	253.8	-	0.02	254.36	-	0.02
0.5	287.61	-	0.21	269.90	-	0.06
0.6	304.92	-	0.52	312.57	-	0.80
0.7	315.55	-	0.81	317.29	-	0.89
0.8	320.25	-	0.92	319.55	-	0.88
0.9	322.20	-	0.91	323.40	-	0.97
1.0	326.10		1.00	326.10		1.00

Table S2. Melting temperature (T_m) and melting enthalpy (ΔH_m) for the HES pure components

Component	T_m **(K)**	ΔH_m **(kJ·mol^{-1})**	**Reference**
TOPO	326.1	45.7	Measured
AceA	289.8	10.83	[1]
HexA	269.2	16.40	[2,3]
DecA	304.8	27.50	[4]

SOLVENT EXTRACTION

Table S3. Distribution factors of five lanthanide cations, in the TOPO + $C_nH_{(2n+1)}COOH$ systems (n = 1, 5, or 9) as a function of the HES x_{TOPO} molar fraction for $[HNO_3]$ = 1.0 mol·L^{-1}, T = 298 K, $[Ln^{3+}]$ = 7.5 mmol·L^{-1}, and O/A = 0.5.

HBD	x_{TOPO}	D_{La}	D_{Nd}	D_{Eu}	D_{Tb}	D_{Lu}
AceA	0.3	7.85 ± 0.35	50.8 ± 0.81	79.3 ± 1.76	103 ± 0.50	47.9 ± 0.64
	0.5	7.27 ± 0.03	25.1 ± 0.73	107 ± 2.47	104 ± 1.01	19.8 ± 0.23
HexA	0.3	0.04 ± 0.01	0.19 ± 0.02	0.69 ± 0.11	0.77 ± 0.01	0.48 ± 0.01
	0.5	0.87 ± 0.01	6.29 ± 0.06	15.6 ± 0.73	14.9 ± 0.10	4.46 ± 0.03
DecA	0.3	0.19 ± 0.02	0.20 ± 0.04	0.23 ± 0.02	0.19 ± 0.09	0.25 ± 0.05
	0.5	1.00 ± 0.12	3.16 ± 0.22	8.16 ± 0.19	7.43 ± 0.26	6.72 ± 0.28

Table S4. Distribution factors of five lanthanide cations, in the TOPO + $C_nH_{(2n+1)}COOH$ systems (n = 1, 5, or 9) as a function of the HES x_{TOPO} molar fraction for $[HNO_3]$ = 6.0 mol·L^{-1}, T = 298 K, $[Ln^{3+}]$ = 7.5 mmol·L^{-1}, and O/A = 0.5.

HBD	x_{TOPO}	D_{La}	D_{Nd}	D_{Eu}	D_{Tb}	D_{Lu}
AceA	0.3	0.62 ± 0.09	1.13 ± 0.09	1.43 ± 0.12	1.45 ± 0.10	5.21 ± 0.14
	0.5	0.21 ± 0.05	0.47 ±0.05	1.03 ± 0.05	0.66 ± 0.03	2.33 ± 0.03
HexA	0.3	0.17 ± 0.04	0.10 ± 0.06	0.12 ± 0.05	0.15 ± 0.01	1.32 ± 0.26
	0.5	0.10 ± 0.03	0.17 ± 0.13	0.55 ± 0.01	1.22 ± 0.06	0.90 ± 0.01
DecA	0.3	0.11 ±0.07	0.11 ± 0.14	0.04 ± 0.03	0.08 ± 0.04	0.87 ± 0.08
	0.5	0.45 ± 0.01	0.41 ± 0.50	0.47 ± 0.07	0.54 ± 0.03	1.56 ± 0.11

Table S5. Separation factor D_{Eu} / D_{Ln} in the TOPO + $C_nH_{(2n+1)}COOH$ systems (n = 1, 5, or 9) as a function of the HES x_{TOPO} molar fraction for $[HNO_3]$ = 1.0 mol·L^{-1}, T = 298 K, $[Ln^{3+}]$ = 7.5 mmol·L^{-1}, and O/A = 0.5.

HBD	x_{TOPO}	D_{Eu} / D_{La}	D_{Eu} / D_{Nd}	D_{Eu} / D_{Tb}	D_{Eu} / D_{Lu}
AceA	0.3	10.13	1.57	0.77	1.66
	0.5	14.72	4.27	1.03	5.40
HexA	0.3	19.87	3.62	0.90	1.44
	0.5	17.91	2.48	1.05	3.49
DecA	0.3	1.23	1.15	1.21	0.92
	0.5	8.16	2.58	1.10	1.21

Table S6. Separation factor D_{Eu} / D_{Ln} in the TOPO + $C_nH_{(2n+1)}COOH$ systems (n = 1, 5, or 9) as a function of the HES x_{TOPO} molar fraction for $[HNO_3]$ = 6.0 mol·L^{-1}, T = 298 K, $[Ln^{3+}]$ = 7.5 mmol·L^{-1}, and O/A = 0.5.

HBD	x_{TOPO}	D_{Eu} / D_{La}	D_{Eu} / D_{Nd}	D_{Eu} / D_{Tb}	D_{Eu} / D_{Lu}
AceA	0.3	2.30	1.26	0.99	0.27
	0.5	4.90	2.19	1.57	0.44
HexA	0.3	0.72	1.25	0.85	0.09
	0.5	5.78	3.26	0.45	0.61
DecA	0.3	0.32	0.33	0.43	0.04
	0.5	1.03	1.13	0.87	0.30

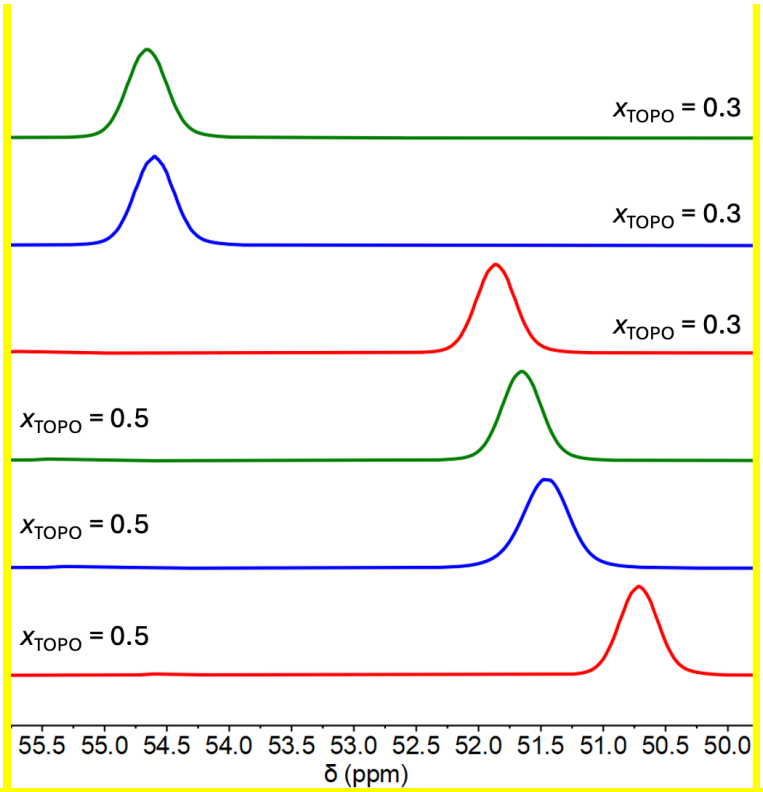


Figure S1. ^{31}P-NMR spectra of TOPO in the TOPO + $C_nH_{(2n+1)}COOH$ systems (n = 1, 5, or 9) after equilibration with H_2O in the absence of metal salts (O/A=0.5, 298.15 K) as a function of the HBD selection (AceA – red, HexA – blue, DecA – green) and x_{TOPO}.

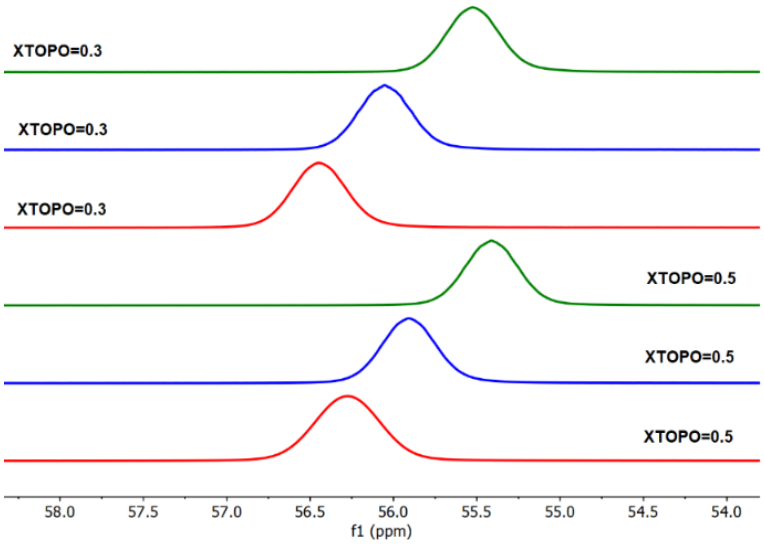


Figure S2. ^{31}P-NMR spectra of TOPO in the TOPO + $C_nH_{(2n+1)}COOH$ systems (n = 1, 5, or 9) after equilibration with 1.0 mol·L^{-1} HNO_3 in the absence of metal salts (O/A=0.5, 298.15 K) as a function of the HBD selection (AceA – red, HexA – blue, DecA – green) and x_{TOPO}.

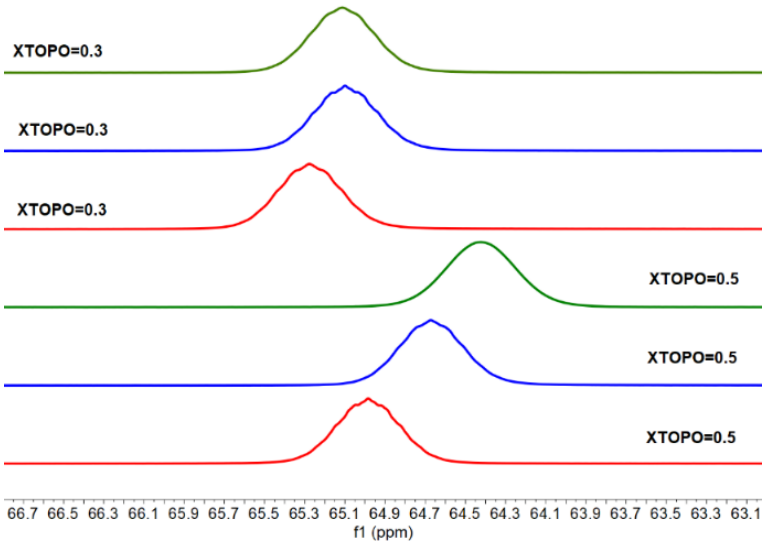


Figure S3. ^{31}P-NMR spectra of TOPO in the TOPO + $C_nH_{(2n+1)}COOH$ systems (n = 1, 5, or 9) after equilibration with 6.0 mol·L^{-1} HNO_3 in the absence of metal salts (O/A=0.5, 298.15 K) as a function of the HBD selection (AceA – red, HexA – blue, DecA – green) and x_{TOPO}.

LOADING CAPACITY

Table S7. $Eu(NO_3)_3$ loading test in the TOPO + $C_nH_{(2n+1)}COOH$ systems (n = 1, 5, or 9) and corresponding viscosity of the phase as a function of the HBD selection and x_{TOPO}, after equilibration with an $[Eu^{3+}]_{aq,ini}$ = 0.2 mol·L^{-1} solution at 1.0 mol·L^{-1} NO_3^- and O/A = 0.5. The concentration of bound TOPO to Eu^{3+} was calculated from the total TOPO concentration in the HES, the final extracted Eu^{3+} concentration and assuming a 3:1 TOPO:Eu stoichiometry of the complex.

HBD	x_{TOPO}	$[Eu]_{HES,f}$ (g·kg^{-1})	E (%)	$[TOPO]_{Bound}$ (mol·kg^{-1})	η (mPa·s)
AceA	0.3	55.7 ± 0.16	82.4	1.00	219 ± 8.2
	0.5	53.22 ± 0.04	78.7	0.96	228 ± 18.2
HexA	0.3	10.3 ± 0.11	64.3	0.18	29.9 ± 1.41
	0.5	31.0 ± 0.11	13.8	0.55	41.4 ± 1.11
DecA	0.3	9.09 ± 0.61	53.0	0.16	44.1 ± 0.1
	0.5	15.7 ± 1.43	7.26	0.27	86.0 ± 0.9

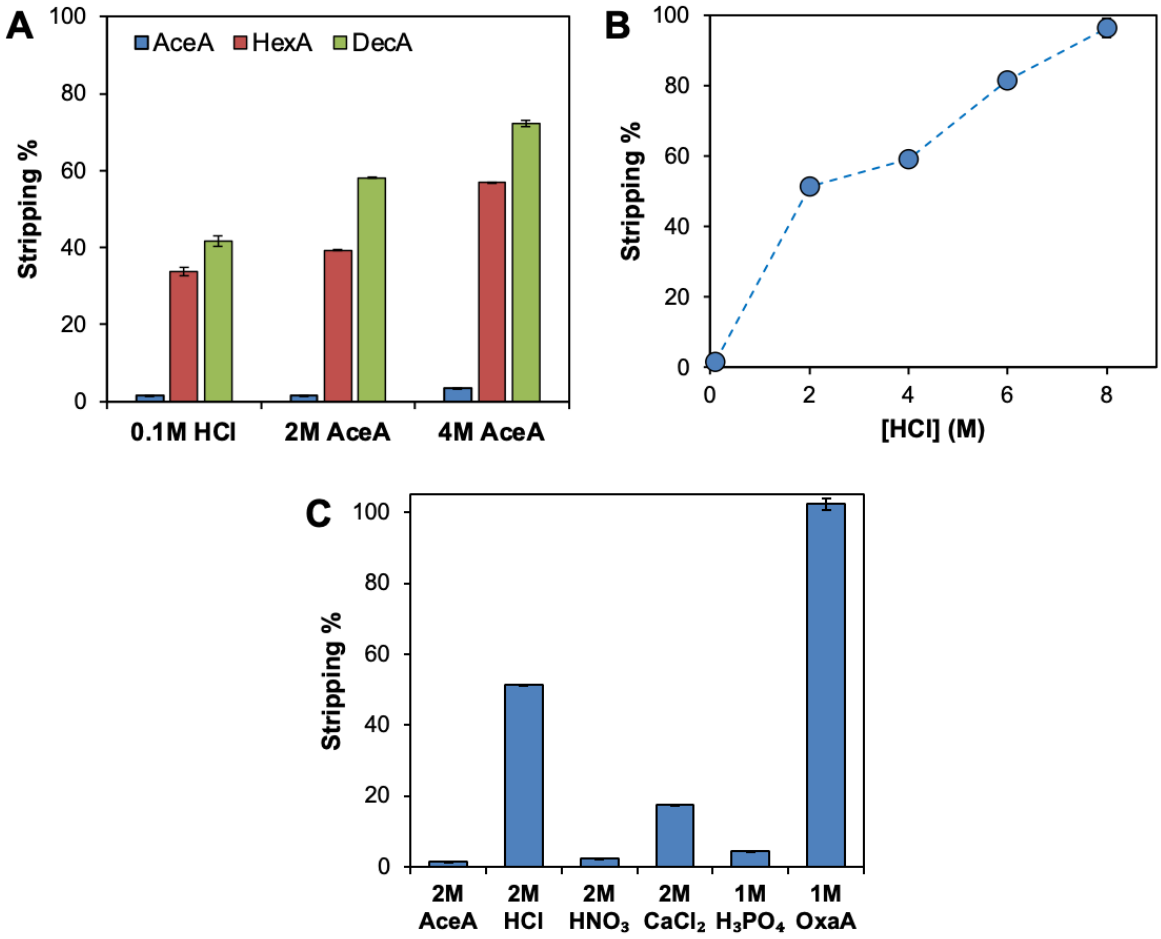


Figure S4. Stripping efficiency (%) of Eu^{3+} from the loaded TOPO + $C_nH_{(2n+1)}COOH$ systems (n = 1, 5, or 9) as a function of A) HBD selection, B) HCl concentration from the TOPO + AceA system, and C) stripping phase composition from the TOPO + AceA system. Constant stripping conditions of O/A= 0.5 and *T*= 298.15 K were maintained.

LUMINESCENCE MEASUREMENTS

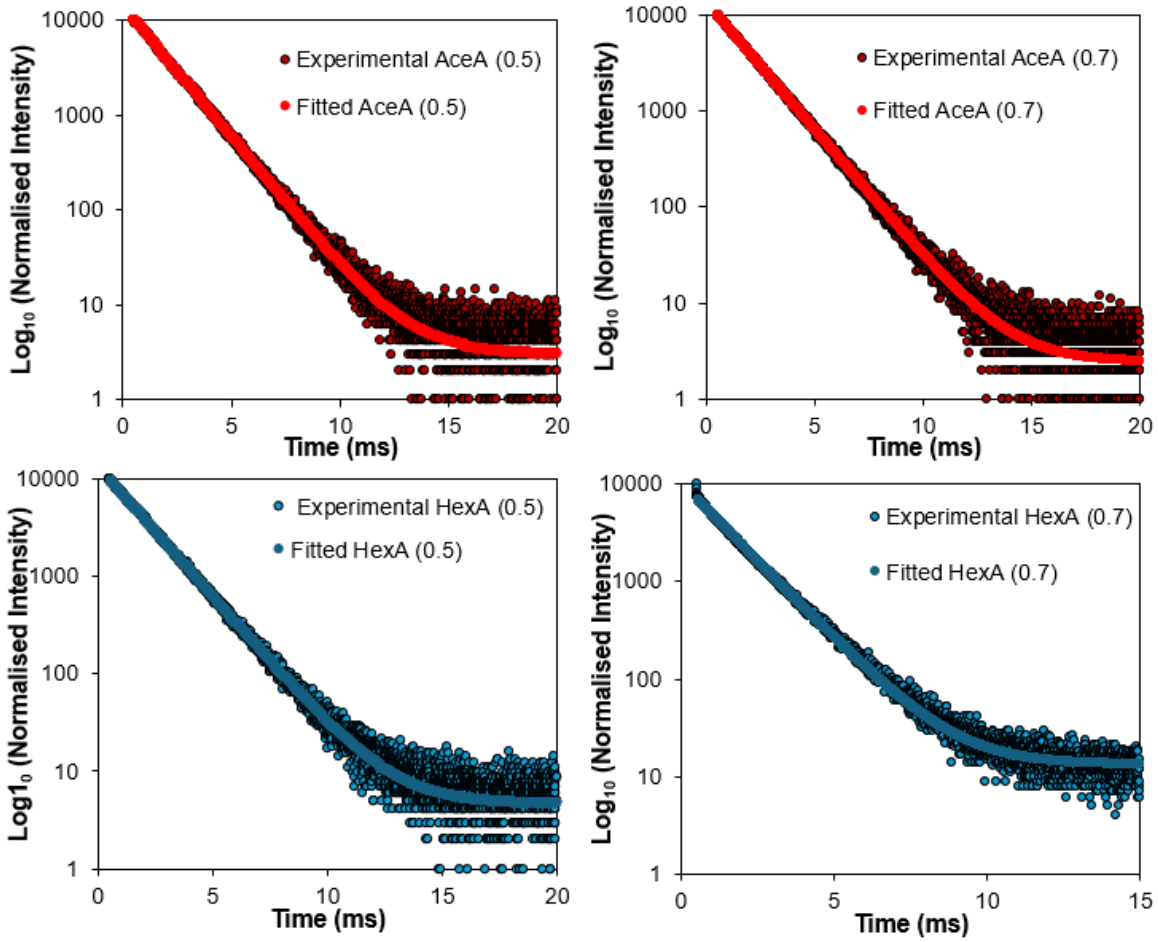


Figure S5. Normalized Eu^{3+} $^5D_0$ decay curves detecting the emission at 617.4 nm, using the SpectraLED-355 as excitation source, as a function of HBD selection and x_{TOPO} in the TOPO + carboxylic acid systems with H_2O, along with the single exponential decay fit. SX conditions are equal to those in **Figure 4** of the manuscript.

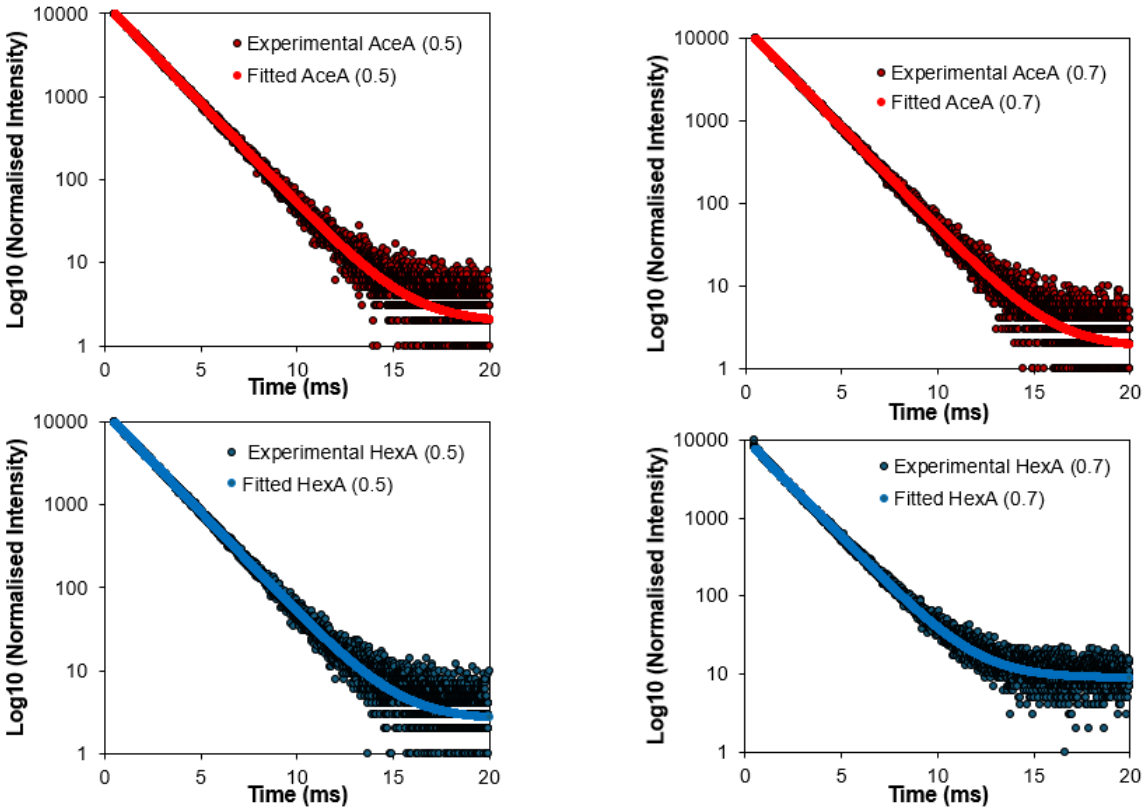


Figure S6. Normalized Eu^{3+} $^5D_0$ decay curves detecting the emission at 617.4 nm, using the SpectraLED-355 as excitation source, as a function of HBD selection and x_{TOPO} in the TOPO + carboxylic acid systems with D_2O, along with the single exponential decay fit. SX conditions are equal to those in **Figure 4** of the manuscript.

POLAR SOLUTE CO-EXTRACTION

Table S8. Polar solute concentration in the HES phase as a function of the HBD and x_{TOPO} after equilibration with an aqueous phase of H_2O or 1.0 mol·L^{-1} HNO_3 in the absence of Ln^{3+} ions at O/A = 0.5 and T = 298 K. The associated error with the determination of HBD loss in 1.0 mol·L^{-1} HNO_3 meant these were only determined after contact with H_2O.

HBD	x_{TOPO}	H_2O aqueous phase		1.0 mol·L^{-1} HNO_3 aqueous phase	
		$[H_2O]_{HES,f}$ (mol·kg^{-1})	$[HBD]_{aq,f}$ (mol·kg^{-1})	$[H_2O]_{HES,f}$ (mol·kg^{-1})	$[HNO_3]_{HES,f}$ (mol·kg^{-1})
AceA	0.3	2.26 ± 0.15	1.03 ± 0.04	1.64 ± 0.09	0.832 ± 0.085
	0.5	1.80 ± 0.12	0.35 ± 0.03	1.52 ± 0.28	0.818 ± 0.058
HexA	0.3	1.53 ± 0.12	0.027 ± 0.009	0.91 ± 0.21	0.395 ± 0.028
	0.5	1.47 ± 0.24	0.007 ± 0.001	1.07 ± 0.34	0.492 ± 0.056
DecA	0.3	1.31 ± 0.24	0.001 ± 0.001	0.58 ± 0.04	0.209 ± 0.029
	0.5	1.07 ± 0.09	0.001 ± 0.001	0.75 ± 0.02	0.360 ± 0.074

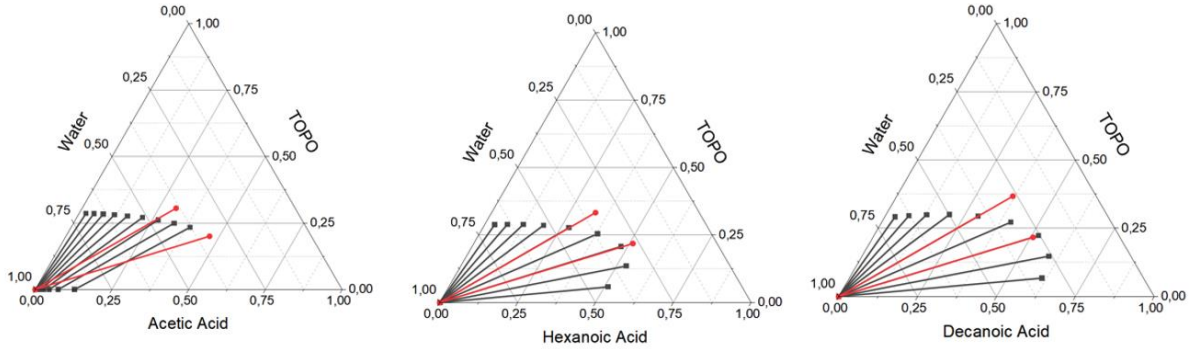


Figure S7. Comparison of the experimental (red) and COSMO-RS predicted (black) liquid-liquid phase diagram of the ternary water/TOPO/HBD system (in molar fraction) as a function of the HBD alkyl chain length for T = 298.15 K.

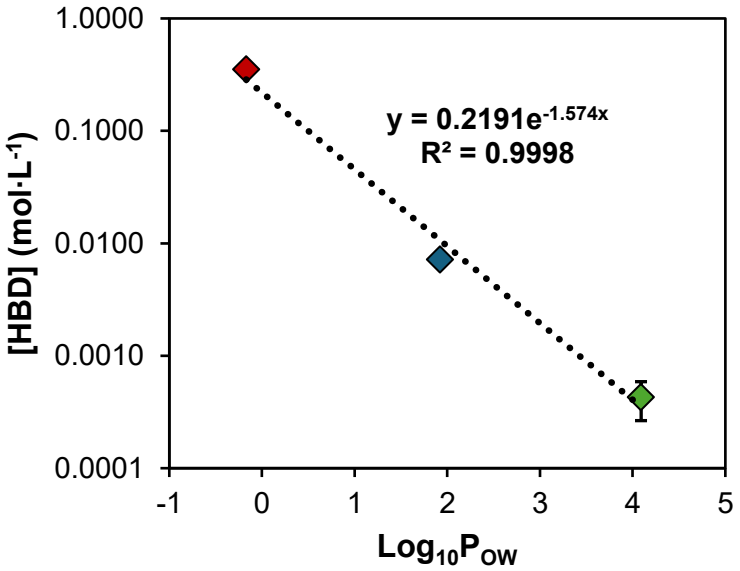


Figure S8. Aqueous phase concentration of the carboxylic acid (AceA, HexA, and DecA) after equilibration of the TOPO+ Carboxylic acid HES with H_2O as a function of the logarithm of the octanol/water partition ($\log_{10}P_{OW}$) for the three protonated forms of the HBD, taken from ref [5] ($x_{TOPO} = 0.5$, $T = 298$ K, and O/A = 0.5)

MOLECULAR DYNAMIC SIMULATION

Table S9. System composition of the TOPO + AceA and TOPO + DecA systems for x_{TOPO} of 0.3 or 0.5 with increasing water content at 298 K. All systems contain a total of 1000 HES molecules with varying water content. The x_{TOPO} corresponds to the HES composition before water addition. V_{box} corresponds to the final simulation box volume, whilst N_{domain} and V_{domain} correspond to the time averaged polar domain number and polar domain volume. All analysis was carried out on the last 20 ns of the simulation run. Polar domain is defined as the P=O group of TOPO, COOH group of the carboxylic acid, and water molecules.

HBD	x_{TOPO}	n(TOPO)	n(HBD)	n(H_2O)	[H_2O] (mol.%)	[H_2O] (wt.%)	V_{box} (nm^3)	V_{domain} (nm^3)	N_{domain}
AceA	0.3	300	700	0	0.0	0.0	6.602	7.57	10.9
	0.3	300	700	500	33.3	5.4	6.715	20.2	5.5
	0.5	500	500	0	0.0	0.0	7.468	0.43	147
	0.5	500	500	100	9.1	0.8	7.487	0.57	116
	0.5	500	500	300	23.1	2.4	7.521	0.93	77
	0.5	500	500	500	33.3	3.9	7.557	1.41	55
DecA	0.3	300	700	0	0.0	0.0	7.619	0.105	362
	0.3	300	700	300	23.1	2.2	7.674	0.178	261
	0.5	500	500	0	0.0	0.0	8.076	0.074	485
	0.5	500	500	100	9.1	0.6	8.091	0.088	443
	0.5	500	500	300	23.1	1.9	8.123	0.118	376

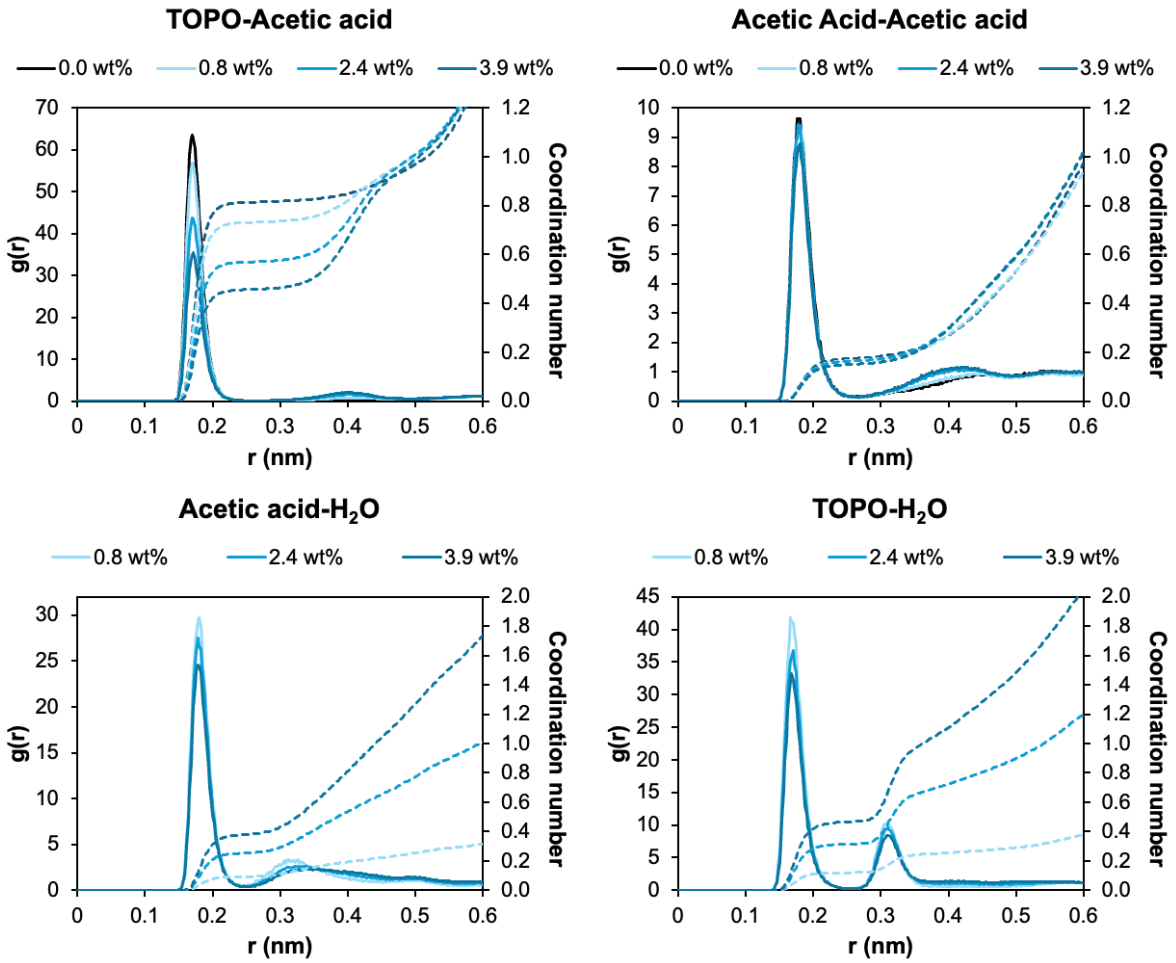


Figure S9. Radial distribution functions (RDFs) and associated coordination number for TOPO + AceA system with increasing of water content for an initial x_{TOPO} = 0.5. The x_{TOPO} corresponds to the HES composition before water addition.

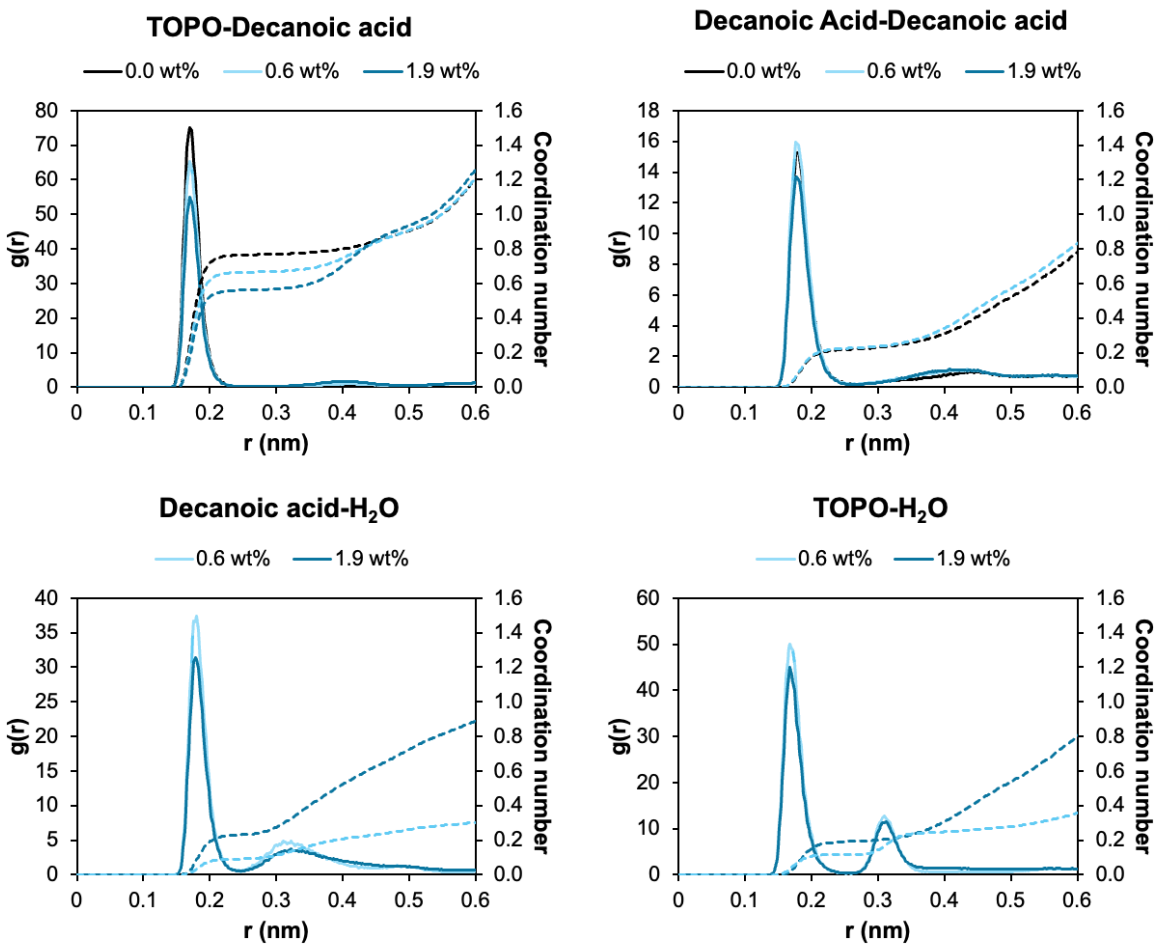


Figure S10. Radial distribution functions (RDFs) and associated coordination number for TOPO + DecA system with increasing of water content for an initial x_{TOPO} = 0.5. The x_{TOPO} corresponds to the HES composition before water addition.

TERNARY SYSTEMS

Table S10. Polar solute concentration (mol·kg^{-1}) in the ternary TOPO/AceA/DecA HES phase as a function of the AceA to DecA molar ratio after equilibration with an aqueous phase of H_2O or 1.0 mol·L^{-1} HNO_3 in the absence of Ln^{3+} ions at O/A = 0.5 and T = 298 K. The associated error with the determination of HBD loss in 1.0 mol·L^{-1} HNO_3 meant these were only determined after contact with H_2O.

$x_{AceA}/(x_{DecA} + x_{AceA})$	**H_2O aqueous phase**		**1.0 mol·L^{-1} HNO_3 aqueous phase**	
	$[HBD]_{aq,f}$	**$[H_2O]_{HES,f}$**	**$[H_2O]_{HES,f}$**	**$[HNO_3]_{HES,f}$**
0.00	0.001 ± 0.001	1.07 ± 0.09	0.75 ±0.02	0.36 ± 0.07
0.25	0.121 ± 0.001	1.29 ± 0.28	0.97 ± 0.10	0.52 ± 0.01
0.50	0.199 ± 0.003	1.70 ± 0.11	1.16 ± 0.13	0.65 ± 0.01
0.75	0.307 ± 0.002	1.84 ± 0.13	1.39 ± 0.12	0.78 ± 0.01
1.00	0.350 ± 0.030	1.80 ± 0.12	1.52 ± 0.28	0.82 ± 0.06

Reference

[1] G.S. Parks, K.K. Kelley, Thermal data on organic compounds. II. The heat capacities of five organic compounds. The entropies and free energies of some homologous series of aliphatic compounds, J. Am. Chem. Soc. 47 (1925) 2089–2097. https://doi.org/10.1021/ja01685a003.

[2] J.M. Costello, S.T. Bowden, The temperature variation of orthobaric density difference in liquid-vapour systems. IV. Fatty acids, Recueil Des Travaux Chimiques Des Pays-Bas 77 (1958) 803–810. https://doi.org/10.1002/recl.19580770903.

[3] L. Müller, G. Rubio-Pérez, A. Bach, N. Muñoz-Rujas, F. Aguilar, J. Worlitschek, Consistent DSC and TGA Methodology as Basis for the Measurement and Comparison of Thermo-Physical Properties of Phase Change Materials, Materials 13 (2020) 4486. https://doi.org/10.3390/ma13204486.

[4] P.V.A. Pontes, E.A. Crespo, M.A.R. Martins, L.P. Silva, C.M.S.S. Neves, G.J. Maximo, M.D. Hubinger, E.A.C. Batista, S.P. Pinho, J.A.P. Coutinho, G. Sadowski, C. Held, Measurement and PC-SAFT modeling of solid-liquid equilibrium of deep eutectic solvents of quaternary ammonium chlorides and carboxylic acids, Fluid Phase Equilib. 448 (2017) 69–80. https://doi.org/10.1016/j.fluid.2017.04.007.

[5] J. Sangster, Octanol-Water Partition Coefficients of Simple Organic Compounds, J. Phys. Chem. Ref. Data 18 (1989) 1111–1229. https://doi.org/10.1063/1.555833.